Applied Clay Science 288 (2026) 108232

Contents lists available at ScienceDirect

Applied Clay Science

journal homepage: www.elsevier.com/locate/clay

Research Paper

A comprehensive characterization of sepiolite clays for isopropanol dehydration to propylene

Tien Hoang Nguyen [a], Jean-Luc Dubois [b], Aline Auroux [a], Georgeta Postole [a,*]

[a] Université Lyon 1, CNRS, IRCELYON, UMR, 5256 Villeurbanne, France
[b] Trinseo Netherlands B.V., Innovatieweg 14, 4542 NH Hoek, the Netherlands

ARTICLE INFO

Keywords:
Sepiolite
Clay catalyst
Isopropanol dehydration
Acid sites
Aluminum

ABSTRACT

This study highlights the potential of natural sepiolites, abundant fibrous hydrated magnesium silicates, as possible eco-friendly acid catalysts. By investigating materials with different aluminum contents, their thermal behavior up to 600 °C and leaching by water or acid treatments, the role of Al^{3+} substituting Si^{4+} or Mg^{2+} in the tunning of acid properties of sepiolites is discussed. The amount, strength and strength distribution of the acid sites were determined by NH_3 adsorption microcalorimetry. Besides, Fourier Transform InfraRed and Nuclear Magnetic Resonance spectroscopy techniques were used to get insight into the nature of the acid sites when low amount of Al is incorporated in the sepiolite structure. The density of acid sites, key parameter for high catalytic activity, increased with the Al content. Bridging silanol (Si–O[H^+]-Al) Brønsted acid sites were evidenced in thermally treated samples. Isopropanol conversion was studied between 100 and 300 °C in a pulse system for its practical importance for green propylene production and as test reaction to probe the acid properties of solids. The edge Al^{VI} species able to reversibly reduce their coordination number under the reaction conditions and medium strengths sites (80 to 150 kJ/mol as determined by NH_3 adsorption microcalorimetry) are at the origin of active acid sites.

1. Introduction

Clay minerals are finding growing applications across a range of domains due to their natural abundance and favorable properties. Their mineralogical composition and structure give rise to their physico-chemical properties, including the ability to swell in water, cation-exchange capacity, high surface area, and multimodal porous structure. Moreover, such features can be readily managed and enhanced through diverse purification, activation, or modification methods without greatly damaging their intrinsic structure and composition. Given their surface properties and low cost, clays are increasingly compelling for a variety of domains such as agriculture, environmental remediation (Bergaya and Lagaly, 2013; Ouali et al., 2015), and catalysis (Figueras, 1988; Belaroui and Benguedach, 2012; Al-Ani et al., 2018; Abeyta et al., 2024).

The sepiolite clay, $Si_{12}O_{30}Mg_8(OH)_4(OH_2)_4{\cdot}8H_2O$, possibly containing partial aluminum substituted to magnesium and silicium, is classified within the sheet-silicate (phyllosilicate) group, alongside palygorskite (Al-Ani et al., 2018). The structural blocks comprise two tetrahedral silica sheets inverting from one sheet to the other and sandwiching a central discontinuous octahedral sheet of magnesium oxide-hydroxide. This configuration gives to sepiolite a unique tunnel-like structure compared to the other types of clay minerals and makes it a suitable adsorbent and catalyst support (Aramendía et al., 1997; Portela et al., 2015; Balestra et al., 2023). In the past decade, the application of sepiolite for battery materials has also emerged (Chen et al., 2018).

Having a configuration containing tetrahedral silica layers, sepiolite can possibly possess acid sites like other well-known silica-based or zeolite materials. Nevertheless, the acidity of sepiolite catalysts has not been extensively studied. For instance, the presence of Al^{3+} substituting tetrahedral Si^{4+} can induce bridging-silanol [Si-O(H^+)-Al] Brønsted acid sites (Chizallet and Raybaud, 2009, 2010; Larmier et al., 2017). This hypothesis has not been thoroughly explored in the case of sepiolite, despite being evidenced in other clay materials namely montmorillonite (Plee et al., 1985), beidellite (Plee et al., 1987) and saponite (Chevalier et al., 1994). Besides, at the edges of intermittent octahedral ribbons, water molecules complete the coordination of octahedral Mg^{2+} cations or Al^{3+} cations (if there is a substitution of Mg^{2+} by Al^{3+} at that position). The Al-coordinated water molecules species are at the origin of

* Corresponding author.
E-mail address: georgeta.postole@ircelyon.univ-lyon1.fr (G. Postole).

https://doi.org/10.1016/j.clay.2026.108232
Received 19 December 2025; Received in revised form 1 April 2026; Accepted 4 April 2026
Available online 8 April 2026

Brønsted acidity in Al-exchanged sepiolite due to their strong polarization by Al^{3+} which facilitates proton donation (Corma et al., 1984). At temperatures above 250 °C, these water molecules are lost and thus possibly creating coordinatively unsaturated Al^{V} sites, acting as Lewis acid sites (D'Espinose De La Caillerie and Fripiat, 1992).

Several studies have been carried out by Corma et al. (Corma et al., 1984, 1985) to assess the acidity of sepiolite using pyridine adsorption-FTIR. Their primary objective was to gain an overall understanding of sepiolite's potential in the catalyst industry. It was reported that sepiolite has a limited amount of Lewis and/or Brønsted acid sites. The authors proposed that the origin of the Brønsted acidity lays in the polarized Al-coordinated-water molecules at the edge of the octahedral layer. D'Espinose De La Caillerie and Fripiat (D'Espinose De La Caillerie and Fripiat, 1992) investigated Al-modified sepiolite as catalyst support. By using solid state ^{27}Al NMR spectroscopy, coordinatively unsaturated Al^{V} sites were revealed in the material calcined at 450 °C without correlation to any specific acid-catalyzed reaction. Further, the authors (D'Espinose De La Caillerie et al., 1995; Sun et al., 1995) attempted to modify sepiolite by Al substitution methods for catalysis application expecting to observe Brønsted acid sites generated from the substitution in tetrahedral layer. However, contradictory to their assumption, only Lewis acid sites were induced due to the substitution in octahedral layers. Zhou et al. (Zhou et al., 2017) and Marosz et al. (Marosz et al., 2020) studied the activation/modification of sepiolite for acid-catalyzed alcohol dehydration reactions. Their main aim was to find suitable activation conditions without going further in the correlation between the activated clays properties and their catalytic performances. Belver et al. (Belver et al., 2013) synthesized silica-alumina-organosepiolite composites for isopropanol dehydration reaction. In their study, the catalytic activity was demonstrated to come from silica-alumina phase, tuned by the variation of Si/Al ratio and sepiolite only served as a fibrous template for anchoring silica-alumina particles, allowing the formation of porous nanoarchitectures. Chen et al. (Chen et al., 2021) studied the structure and properties of sepiolite with different percentages of Al-substitution in the structure, but with the aim to investigate the bonding strength of Al-sepiolite with indigo dye for pigment applications.

The decomposition of isopropanol (IPA) through dehydration or dehydrogenation is a well-known model reaction for studying catalyst acid-base properties (Dubois et al., 2022). A significant challenge in using the IPA dehydration reaction for propylene production is to avoid the formation of unwanted by-products, mainly di-isopropyl ether (DIPE) and acetone (ACE). DIPE forms at high operation pressures and in a lower range of temperatures, requiring both basic and acidic sites. Acetone is produced via isopropoxide species at basic sites, which can lead to side reactions (Dubois et al., 2022). Achieving high-quality polymer-grade propylene requires very fine catalyst selection and optimal reaction conditions, emphasizing low basicity to minimize by-products formation (Gervasini et al., 1997; Dubois et al., 2022). Several decades ago, studies focused on simpler catalysts like mixed oxides and zeolites, and recently, formulas containing zirconium and gallium have appeared (Dubois et al., 2022). However, the adoption of these catalysts is limited by their reliance on critical raw materials and potentially toxic chemicals. In 2011, Mitsui developed an IPA process using γ-Al_2O_3 (Fukuhara et al., 1989). Other patented methods from IFPEN (Aribert et al., 2014) and Versalis (Fois and Buzzoni, 2018) also employ alumina and large-pore zeolites for propylene production. Extending the research on natural and abundant materials such as clays will further expand the industrial feasibility of the production of high-grade propylene. The use of clays as acid catalysts instead of other conventional materials is also advantageous due to their low environmental impact, helping reducing the ecological footprint and promoting more sustainable practices in the industry (Abeyta et al., 2024). Although the presence of silanol groups can generate intrinsic weak acidity in sepiolite and may promote acid-catalyzed reactions to a certain extent, the role of trivalent substitution in governing the acidity of sepiolite remains particularly significant and worthy of detailed investigation. Up to date, limited studies report systematic acidity characterization (nature, number, strength and strengths distribution) of sepiolites with respect to their potential use in acid-catalyzed reactions. According to Phung et al. (Phung and Busca, 2015), for zeolite materials, when the Al percentage is relatively low, the amount of acid sites is strictly dependent on Al concentration.

In this context, the aim of the present work was to study the impact of the structural and acid properties of low content Al-sepiolites on their performances in the catalytic dehydration of isopropanol to propylene. Sepiolite was chosen because its widespread occurrence among the natural clay minerals and its promising catalytic properties for dehydration reactions (Corma and Pérez-Pariente, 1987). Special emphasis was placed on the role of Al content and coordination environment in providing active sites and governing the acidity of sepiolite. To this end, leaching experiments by water (liquid phase) or acid treatments were carried out to tune the amount and the distribution of Al sites in the sepiolite structure. All studied materials were then characterized by X-ray diffraction (XRD), Inductively coupled plasma optical emission spectrometry (ICP-OES), ^{27}Al magic angle spinning nuclear magnetic resonance (MAS NMR), and N_2 sorption isotherms. The acid properties were investigated by complementary techniques such as NH_3 adsorption microcalorimetry, NH_3 adsorption FTIR, and ^{1}H MAS NMR. The basicity was evaluated by SO_2 adsorption microcalorimetry. The structure−activity relationship of sepiolite catalysts with different Al contents was studied in the catalytic dehydration of isopropanol (IPA) to propylene (PEN) using a pulse system.

This work demonstrates that sepiolite clays, due to their mesoporous character and medium strength acidity, are promising natural catalysts for propylene production from isopropanol affording good activity and selectivity at temperatures as low as 150 °C (at low partial pressure). The relationship between the density of acid sites and activity is discussed based on the Al content in clays.

2. Materials and methods

2.1. Materials

Three sepiolite clays, in the form of yellowish fine powder, with different contents of Al in the structure were used as kindly supplied by TOLSA (Vallecas, Spain). They belong to the series of commercialized Pangel S (>85% sepiolite, >90% particle size of <5 μm). Catalysts were named 0.9Al-Sep, 1.2Al-Sep, and 1.8Al-Sep with the numbers indicating the Al wt% in the catalysts as determined by ICP-OES. The cation exchange capacities were given as 10, 18 and 12 ± 2 mEq/100 g, respectively. The composition of 0.9Al-Sep is similar with that reported by Pérez-Pariente and Corma (Pérez Pariente et al., 1988) as a natural, untreated sepiolite clay and can be taken as reference material in this study, as being the less acidic. All samples showed fibrous morphology with variable length but with similar thickness as illustrated in Fig. S1 showing SEM/TEM micrographs.

To assess the effect of aluminum on acidity and activity, 1.8Al-Sep was hydrothermally or acid treated. A slurry of 1 g solid in 10 mL solution was refluxed for 2 h at 100 °C (water) or 80 °C (acid, 2 M H_3PO_4.). The resulting suspensions were filtered, washed to neutrality (for acid-treated sample), and dried at 100 °C overnight. The treated samples were denoted Water-1.8Al-Sep and Acid-1.8Al-Sep.

2.2. Characterization methods

Specific surface area and pore volume were determined by N_2 adsorption–desorption at −196 °C employing a TriStar II Plus from Micromeritics. The specific surface area was calculated according to the Brunauer-Emmett-Teller (BET) theory (Brunauer et al., 1938). The pore size and distribution was calculated using the model of Barrett-Joyner-Halenda (BJH) (Barrett et al., 1951). For assessing the effect of

thermally induced structural changes, the samples were outgassed under vacuum (3 h) at temperatures between 200 and 400 °C prior N_2 sorption.

Chemical composition (Si, Mg, Al, Na, Ca, K) was obtained by Inductively Coupled Plasma - Optical Emission Spectrometry- (ICP-OES, Agilent 5800) after acid digestion in HNO_3/HF at 110 °C.

X-ray diffraction (XRD) patterns were recorded by using a Bruker D8 Advance diffractometer (CuKα, λα1 = 1.54060 Å, LynxEye detector) over 2θ = 4–80° (step 0.04°, 0.035 s per step).

Solid-state NMR spectra were acquired on an AVANCE III 500WB: ^{27}Al MAS NMR at 130.29 MHz ($Al(NO_3)_3$ reference; 12 kHz, 1 s, 4096 scans) and ^{1}H MAS NMR at 500.0 MHz (adamantane reference; 12 kHz, 10 s, 16 scans). The samples, pretreated under vacuum, were transferred to the NMR rotor under inert atmosphere.

Thermogravimetric analyses (TGA) were performed on a TGA Discovery from TA Instruments coupled to a Nicolet GX FTIR. The experiments were carried out with 10–12 mg of sample under Ar flow (10 mL/min) from 25 to 600 °C (10 °C/min).

Surface acidity was probed by Fourier transform infrared (FTIR) using NH_3 (15 mbar, 1 h) as probe molecules. Self-supported wafers (30 mg sample, 2 cm^2, placed into a CaF_2-window cell) were calcined and outgassed at 200, 300 and 400 °C before NH_3 adsorption. Spectra were recorded on a Nicolet 8700 (64 scans, 4 cm^{-1}, 1300–4000 cm^{-1}) before and after NH_3 adsorption and further stepwise desorption up to 400 °C.

The amounts, strengths, and strength distributions of acidic and basic sites were determined at 150 °C by means of adsorption microcalorimetry (C80 Tian-Calvet heat flow microcalorimeter from Setaram) linked to volumetry. The detailed methodology can be found in (Auroux, 1994). Ammonia (NH_3) and sulfur dioxide (SO_2) were used to probe acidic and basic sites, respectively. Samples (≈ 0.080 g), pretreated overnight at 400 °C under vacuum, were contacted with successive small doses of probe molecules. After reaching an equilibrium pressure of about 67 Pa the samples were evacuated for 40 min at 150 °C and a second adsorption was performed in order to determine the chemisorption uptakes.

2.3. IPA dehydration: pulse catalytic test

The IPA conversion was assessed in a home-made pulse system at 3 bar and 100–300 °C, using the setup and operating conditions described in (Cabanis et al., 2025). Pulse experiments also allow to evidence the amount of IPA adsorbed on the surface at low temperature. The catalyst (≈15 mg, 300–450 μm) was placed in a microcatalytic pulse reactor inside a calorimeter, and a defined amount of 8% IPA in He (1.15 μmol) was injected via a calibrated loop. The evolution of isopropanol (IPA) conversion and products formation, propylene (PEN), acetone (ACE) and diisopropylether (DIPE), was followed by gas chromatography (Perkin Elmer Clarus 500 GC, Porapak Q column, FID/TCD detector), with chromatograms integrated using OpenChrom. Prior to reaction, the catalysts were pretreated at the desired temperature (200–600 °C) under He flow (30 mL/min) and saturated with IPA at 75 °C, temperature at which no reaction occurs (surface saturation was assumed when successive pulses produced no significant changes in the GC signal). This also allowed examination of the distribution and number of sites interacting with IPA. The catalytic activity of sepiolites was evaluated and compared based on the IPA conversion, PEN yield and PEN selectivity, which were calculated by the equations below, where *n* stands for the number of moles of the substances:

$$IPA\ conversion\ (\%) = \frac{n_{IPA\ in} - n_{IPA\ out}}{n_{IPA\ in}} \times 100$$

$$PEN\ yield\ (\%) = \frac{n_{PEN\ out}}{n_{IPA\ in}} \times 100$$

$$PEN\ selectivity\ (\%) = \frac{n_{PEN\ out}}{n_{IPA\ in} - n_{IPA\ out}} \times 100$$

3. Results and discussion

3.1. Surface area, porosity and chemical composition of the catalysts

The surface area, pore volumes and chemical composition of natural and modified sepiolites are summarized in Table 1. The corresponding nitrogen adsorption–desorption isotherms and pore-size distributions of different catalysts are given in Fig. 1 and Fig. S2.

Among the three pristine samples, 0.9Al-Sep showed the largest surface area and pore volume, followed by 1.2Al-Sep and 1.8Al-Sep. The adsorption isotherms (Fig. 1A) are of a type II (IUPAC). The presence of a hysteresis and the non-parallel N_2 saturation plateau indicate a significant mesopore contribution (Del Rio et al., 2011).

The mesoporous character, with pores up to 50 nm and a maximum around 20 nm (Fig. S2), mainly arised from inter-fiber spaces due to structural defects, while the residual microporosity is associated with tunnels along the fiber c-axis (Ruiz et al., 2023).

The chemical composition of the pristine solids (Table 1) is consistent with the typical structure of sepiolite, composed of tetrahedral silica and octahedral magnesia sheets, in which Al^{3+} ions can substitute for both Si^{4+} in tetrahedral positions and Mg^{2+} in octahedral sites. These substitutions were confirmed by ^{27}Al MAS NMR results (Fig. 1B) of fresh solids. Al^{IV} resonances in the 55–70 ppm range were associated with substitution in the silica tetrahedral sheets and Al^{VI} signals near 0–10 ppm attributed to Al in octahedral environments or extra-layer species (D'Espinose De La Caillerie and Fripiat, 1992; Chen et al., 2021). The relative Al^{IV}/Al^{VI} ratios vary systematically with Al loading and post-treatment (Table S1), reflecting changes in Al coordination induced by hydrothermal and acid treatments. Ca^{2+}, Na^{+}, and K^{+} are likely present as exchangeable cations to compensate for charge deficiencies in the clay framework.

Both water and acid treatments increased the surface area of 1.8Al-Sep (Table 1). This increase, also accompanied for Water-1.8Al-Sep by the mesopore volume rose, is attributed to the removal of impurities or amorphous phases and partial unbundling of sepiolite fibers during vigorous stirring in water at 100 °C, which exposed additional interfibrillar voids. In contrast, the total pore volume remained almost unchanged probably due to partial blockage of micropores by migrating species during treatment. The hydrothermal treatment induced the partial leaching of Al and Mg contents (about 35 and 56%, respectively).

In agreement with previous studies (Plee et al., 1985; Zhou et al., 2017), acid treatment led to a pronounced increase in surface area accompanied by a rise in the total and mesoporous volumes. This behavior is attributed to extensive Mg lixiviation (only trace Mg detected in Acid-1.8Al-Sep, Table 1), which induces leaching of the octahedral sheets and transformation of the structure into amorphous silica phase, as later supported by XRD results (Fig. 2A). The dissolution of the magnesia layers was also accompanied by the loss of more than half of the initial Al content. The remaining aluminum is predominantly present as Al^{IV} species (Table S1) associated with amorphous silica, as observed in the ^{27}Al NMR spectra (Fig. 1B).

3.2. Structure and thermal stability of the catalysts

XRD patterns of the pristine, water-, acid- and thermally- treated samples are shown in Fig. 2A, The untreated samples are characterized by an intense (110) diffraction peak at 2θ = 7.29° (d_{110} ≈ 12.1 Å) similarly to the literature reports (Del Rio et al., 2011; Al-Ani et al., 2018; Pérez Pariente et al., 1988) on natural and Al-modified sepiolites. Other characteristic features of sepiolite ([*] in Fig. 2A) are also observed in addition to reflections from quartz and dolomite impurities. The structure similarity of three untreated samples is further supported by the FTIR spectra when using KBr-support-wafers (Fig. S3 and Table S2) showing the signature peaks of sepiolite.

Water-treated 1.8Al-Sep retains the sepiolite crystalline structure,

Table 1
Surface area, pore volume, and chemical composition of natural and modified sepiolites.

Samples	Surface area and porosity*			Chemical composition (ICP-OES) (wt%)					
	S_{BET} (m^2/g)	$V_{porous\ total}$ (cm^3/g)	$V_{mesoporous}$ (cm^3/g)	Si	Mg	Al	K	Ca	Na
0.9Al-Sep	153	0.48	0.37	20.6	11.5	0.94	0.65	0.54	0.17
1.2Al-Sep	120	0.42	0.34	20.9	11.2	1.24	0.41	0.30	0.09
1.8Al-Sep	108	0.39	0.32	19.8	11.4	1.83	0.57	0.46	0.16
Water-1.8Al-Sep	129	0.39	0.38	25.5	5.02	1.19	0.32	0.14	< 0.01
Acid-1.8Al-Sep	434	0.73	0.64	39.8	0.05	0.85	0.39	0.02	< 0.01

* Samples were outgassed at 300 °C prior to the measurement.

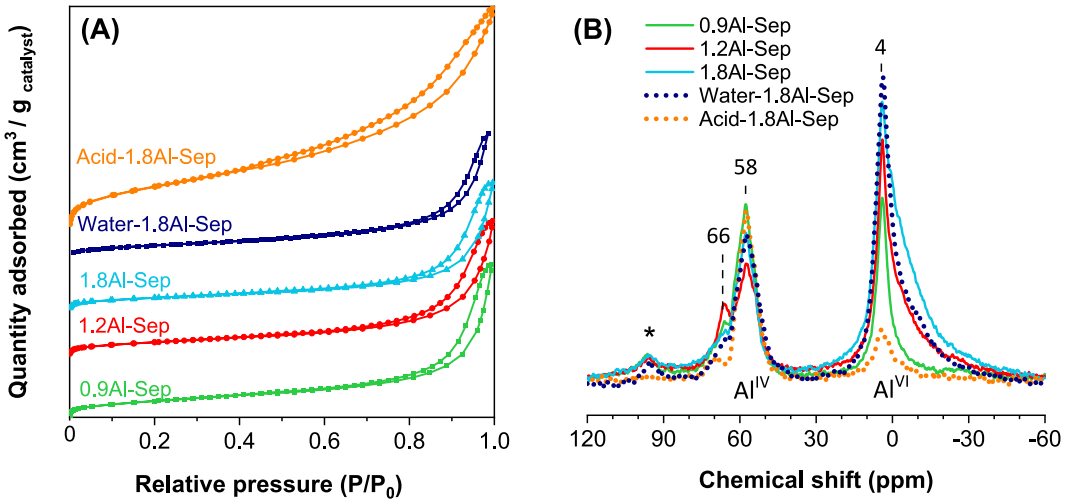

Fig. 1. (A) N_2 adsorption/desorption isotherms at −196 °C and (B) ^{27}Al NMR spectra of the studied catalysts.

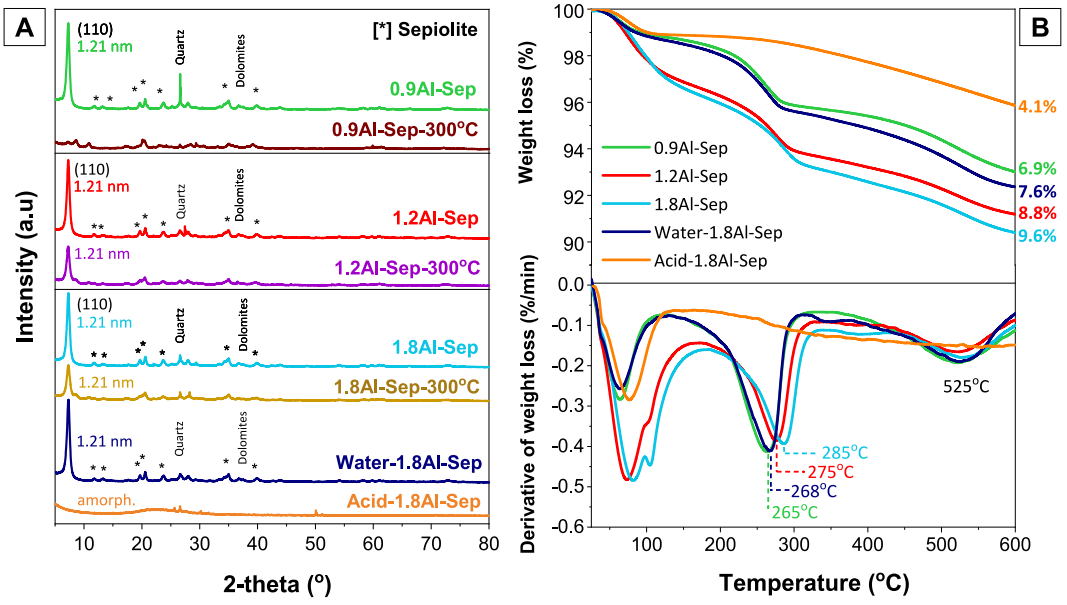

Fig. 2. (A) X-ray diffraction pattern of the pristine, water-, acid- and thermally- treated samples. (B) Main steps of water loss based on thermogravimetric analysis. The raw clay is the untreated 0.9Al-Sep sample.

indicating that partial Mg and Al leaching does not significantly affect long-range order, whereas acid-treated 1.8Al-Sep shows a broad diffraction peak at 2θ = 20–30°, evidencing amorphization due to structural collapse. Thermal treatment at 300 °C does not shift the (110) reflection peak but leads to a marked decrease in its intensity (Fig. 2A). This effect is the most pronounced for the 0.9Al-Sep sample, for which the (110) peak almost disappears, indicating noticeable loss of crystallinity as also observed by Pérez Pariente et al. (Pérez Pariente et al., 1988). 1.2Al-Sep and 1.8Al-Sep clays partially preserved crystallinity, suggesting enhanced thermal resistance with increasing Al contents. The structural degradation observed by XRD is attributed to the loss of coordinated water from the sepiolite framework. A new diffraction feature at 2θ ≈ 8.6° appeared after heating. Although the presence of palygorskite and Mg-smectite as minor components in the sepiolites

cannot be excluded (Casal et al., 1996), the evolution of XRD spectra for heat-treated clays is probably related to the samples folding (Pérez Pariente et al., 1988).

This result is supported by TGA–FTIR analysis (Fig. 2B), which shows stepwise dehydration corresponding to physisorbed water removal below 150 °C followed by the first loss of coordinated water between 180 and 300 °C. The shift to higher temperatures with increasing Al content of the second dehydration step reflects variations in the edge-octahedral composition between clays (D'Espinose De La Caillerie and Fripiat, 1992). Finally, the broader and less intense peak starting from 400 °C corresponds to the second loss of coordinated-water and is associated with significant structural changes in sepiolites (Al-Ani et al., 2018). Indeed, the dehydration-induced structural changes are reversible for samples heated below 400 °C (Fig. S4) which recovered the characteristic two-step coordinated-water loss profile upon rehydration. The surface area and porous volume of sepiolites decreased with increasing heating temperature (Fig. S5 and Table S3).

3.3. Acid-base properties of sepiolites

The quantification of the number, nature, strength, and thermal stability of active sites is crucial for evaluating natural and modified sepiolites as catalysts or catalyst supports. NH_3 adsorption–desorption FTIR experiments reveal the coexistence of Brønsted and Lewis acid sites in all sepiolites (Fig. 3A). Spectra were obtained by subtracting the IR spectra of samples outgassed at 400 °C, from those recorded after NH_3 adsorption (15 mbar, 1 h) and subsequent evacuation at 25 °C (0.5 h).

The band at 3375 cm^{-1} is assigned to NH_3 interacting with exchangeable cations (Ca^{2+}, Na^+, K^+) (Dontsova et al., 2005), while bands at 3193, 3230, 3287, and 1450 cm^{-1} correspond to NH_4^+ species, evidencing Brønsted acidity (Bisio et al., 2008). The shoulder at 1623 cm^{-1} is attributed to NH_3 coordinated to Lewis acid sites (Bisio et al., 2008). This band partially overlaps with the bending vibration of water coordinated to edge octahedral cations (1612–1616 cm^{-1}) (D'Espinose De La Caillerie and Fripiat, 1992), which already exist before NH_3 adsorption.

Untreated pristine samples display distinct acid-sites distributions. 1.2Al-Sep and Water-1.8Al-Sep show similar NH_3 adsorption features, consistent with their comparable surface areas and Al contents. Subtle changes in acid-site distribution induced by hydrothermal treatment cannot be excluded. The 0.9Al-Sep sample, despite the presence of weak NH_4^+ features at 3193, 3230 and 3287 cm^{-1}, exhibits much weaker Brønsted acidity as reflected by a low-intensity band at 1450 cm^{-1}. Acid-1.8Al-Sep shows very low intensities for both Brønsted and Lewis acid characteristic bands, together with the appearance of a band at 1552 cm^{-1} assigned to Si–NH_2 species, indicating extensive structural amorphization and weak acidity.

Desorption experiments reveal a progressive loss of NH_3-related bands with increasing evacuation temperature, with their complete disappearance above 300 °C (Figs. S6–S8), indicating that acid sites are predominantly weak to medium in strength.

The influence of the coordinated-water loss on acidity was examined by varying the outgassing temperature prior to NH_3 adsorption. Taking 1.2Al-Sep as an example (Fig. 3B), increasing the outgassing temperature leads to a clear decrease in NH_4^+ formation, demonstrating a progressive loss of Brønsted acidity. The highest Brønsted acidity is observed with the sample pretreated at 200 °C. The Brønsted sites originate from multiple contributions, including silanol groups, hydronium species associated with negatively charged AlO_4^- units, and water molecules coordinated to unsaturated Al^{3+} at octahedral edges. Due to their high charge density, edge Al^{3+} cations strongly polarize coordinated water (more strongly compared to Mg^{2+}), enhancing its proton-donating ability. Upon further dehydration, Brønsted acidity decreases leading to Lewis acidity generation as evidenced by changes in the 1623 cm^{-1} region. Lewis acid sites arise from coordinatively unsaturated Al centers exposed after the coordinated-water removal and possibly also from dehydrated extra-framework Al species. These observations indicate that the loss of structural water directly govern the Brønsted–Lewis acid balance in sepiolites.

Solid-state ^{27}Al and ^{1}H MAS NMR spectroscopy provide direct structural evidence supporting the acid-site model inferred from the above FTIR results. ^{27}Al MAS NMR spectra in Fig. 4A and Fig. S9 show that tetra-coordinated Al (Al^{IV}, δ ≈ 58 ppm), associated with substitution in the silica framework, remains unchanged upon thermal treatment. In contrast, heating to 400 °C induces partial dehydration of Al-coordinated water, leading to a NMR signal decrease for octahedral Al^{VI} species (δ ≈ 4 ppm) and the emergence of penta-coordinated Al^V species (δ ≈ 29 ppm). These Al^V centers correspond to coordinatively unsaturated Al sites acting as Lewis acid sites due to their ability to accept lone-pair of electrons at the unsaturated position.

Upon partial sepiolite rehydration (sample stored under ambient atmosphere for 24 h) the Al^V signal decreases and Al^{VI} one is partially restored (Fig. 4A), in agreement with TGA findings (Fig. S4). This implies that, water *in situ* generated during the IPA dehydration reaction can re-coordinate to these sites, leading to a dynamic interchange between Brønsted and Lewis acidity. Beside the direct contribution to Lewis acidity, unsaturated Al^V centers can indirectly enhance Brønsted acidity by polarizing neighbor silanol groups, and thus increasing their proton-donating ability. This was previously reported for amorphous silica–alumina and zeolitic systems (Wang et al., 2016), but to our

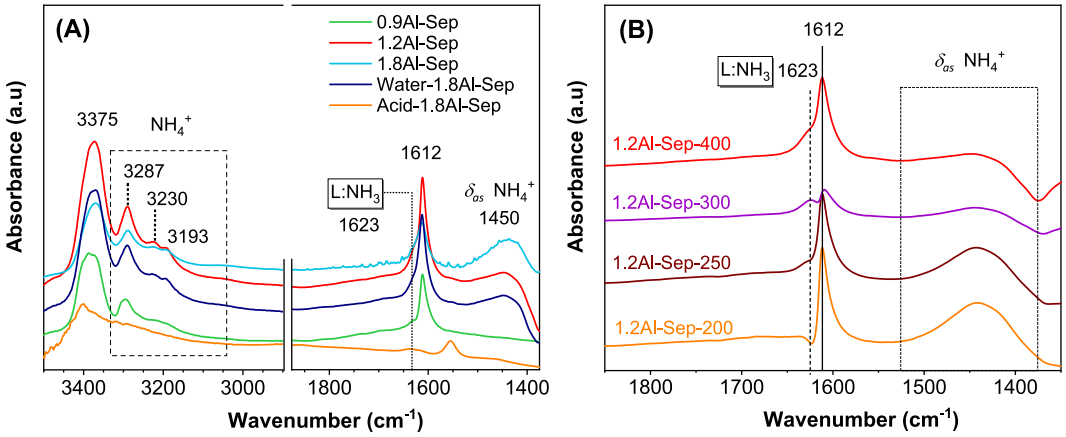

Fig. 3. Subtracted FTIR spectra of NH_3 adsorbed on thermally pretreated catalysts under vacuum: (A) All pretreated at 400 °C and (B) 1.2Al-Sep pretreated at different temperature (200, 250, 300 and 400 °C). All spectra were taken after exposure to 15 mbar of NH_3 for 1 h at 25 °C followed by evacuation at 25 °C for 30 min.

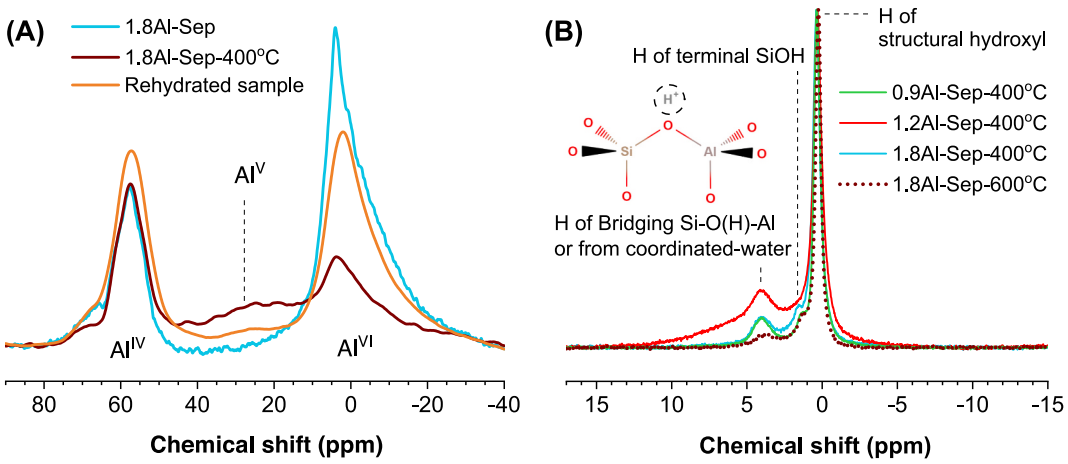

Fig. 4. (A) ^{27}Al NMR spectra of 1.8Al-Sep as received, thermally treated and 400 °C and subsequent rehydration under ambient conditions for 24 h and (B) Solid-state ^{1}H NMR spectra of the thermally treated catalysts.

knowledge, has not been reported in the case of sepiolite.

The quantitative distribution of Al coordination environments before and after thermal treatment is summarized in Table S4.

^{1}H MAS NMR further elucidates the nature of Brønsted acid sites, as shown in Fig. 4B and Fig.S10. Signals at δ ≈ 0.5 ppm arise from structural Mg–OH groups, which are abundant in sepiolites. Band at δ ≈ 1.4 ppm is assigned to terminal silanols acting as weak Brønsted acid sites. The resonance at δ ≈ 4 ppm is associated with Al-coordinated water and/or bridging Si–O(H)–Al Brønsted acid sites (Jiang et al., 2011). To distinguish their contribution, samples outgassed at 600 °C (transferred to NMR rotor under inert conditions to avoid contact with humidity) were analyzed. The results evidence the major contribution of the coordinated-water to the 4 ppm chemical shift for sepiolites treated below 400 °C. But since the coordinated-water is fully desorbed at 600 °C, the residual signal at 4 ppm is exclusively from stable bridging Si–O(H)–Al Brønsted acid sites. To the best of our knowledge, these species have been scarcely reported in the literature on sepiolite materials.

NH_3-FTIR and NMR results demonstrate that water molecules coordinated to Al at octahedral edges play a central role in controlling acid sites distribution in Al-containing sepiolites. As summarized in Fig. 5, sepiolites acidity arises from (i) stable bridging Brønsted sites, (ii) reversibly proton-donating Al-coordinated water, (iii) coordinatively unsaturated Al^{V} Lewis sites formed upon partial sepiolite dehydration above 200 °C, and (iv) dehydrated exchangeable cations or extra-framework Al species. During the reaction, generated water can dynamically rehydrate Al^{V} sites, inducing reversible Brønsted–Lewis interconversion and influence the catalytic behavior. Strong coordinatively-unsaturated Lewis sites may promote side reactions.

The number, strength, and strength distribution of acidic and basic sites were determined by adsorption microcalorimetry using NH_3 and SO_2 as probe molecules, respectively.

Adsorption isotherms (Fig. 6A) exhibit a characteristic initial vertical uptake corresponding to strong irreversible adsorption, followed by a horizontal region associated with pressure-dependent reversible adsorption. Differential heats of adsorption as a function of coverage (Fig. 6B) provide a direct measurement of acid–base strength heterogeneity. The calorimetric and volumetric data for NH_3 adsorption, at 150 °C, are summarized in Table S5.

Sepiolites exhibit a predominantly acidic character, with minor residual basicity attributed to surface O^{2-} anions and hydroxyl groups (e.g., Mg–OH) (Suzuki et al., 1988). Among untreated pristine samples, the reference 0.9Al-Sep shows a higher residual basicity than 1.2Al- and 1.8Al-Sep.

The total acidity varies systematically with Al content and treatment. Based on NH_3 uptake at 150 °C, the amount of accessible acid sites increases in the order of: Acid-1.8Al-Sep < 0.9Al-Sep < Water-1.8Al-Sep ≤ 1.2Al-Sep < 1.8Al-Sep.

The corresponding integral heats of adsorption (Q_{int}) which represent the total heat evolved for the total adsorbed amount at a pressure of 27 Pa are given in Table S5, together with the fraction of occupied sites (calculated as described in (Cabanis et al., 2025)), the acid sites density and the strength distribution. The ratio Q_{int}/V_{total} was calculated and taken as a criterion to compare the average strength of the exposed acid

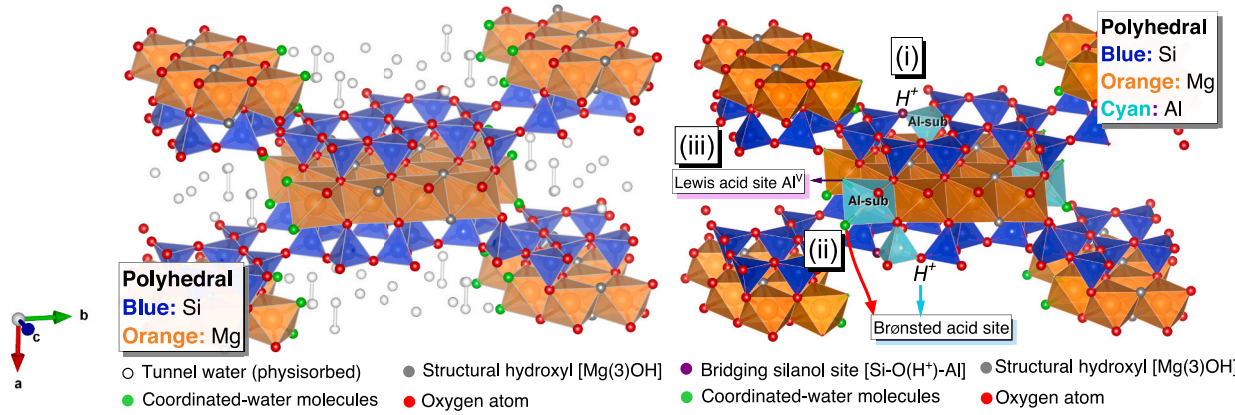

Fig. 5. (Left) Theoretical sepiolite at room temperature versus (right) sepiolite with Al-substitution and pretreated at high temperature (using VESTA software).

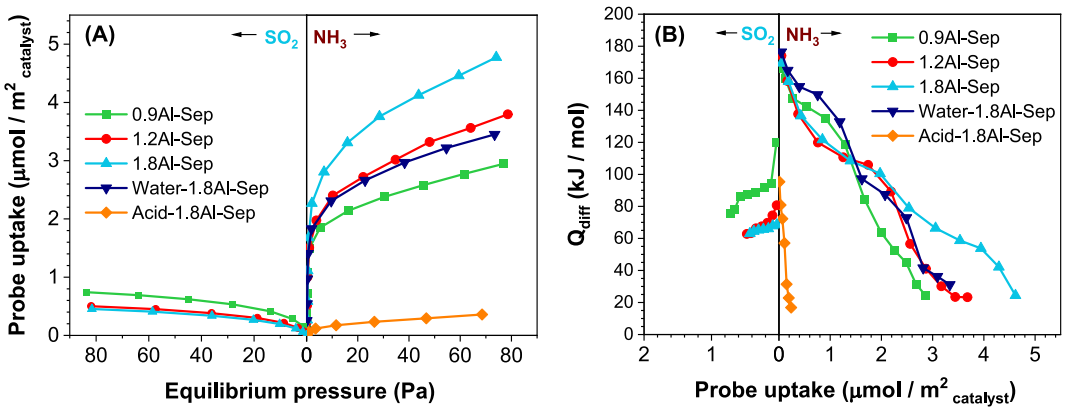

Fig. 6. (A) NH_3 and SO_2 adsorption isotherms at 150 °C of the catalysts. (B) Differential heats of NH_3 and SO_2 adsorption at 150 °C versus coverage.

sites. Similar values were obtained for Water-1.8Al-Sep and 0.9Al-Sep (117 and 112 kJ/mol, respectively) which exhibit slightly stronger sites than 1.2Al-Sep (106 kJ/mol) and 1.8Al-Sep (100 kJ/mol) (Fig. 6B). It can be that the number of medium – weak sites increases with the Al content. Changes in the number and strength of acid sites are observed after acid and water treatments. Acid-1.8Al-Sep has only few weak acidic sites. The amount of adsorbed ammonia decreased after hydrothermal treatment most probably due to partial leaching of Al while the strength of interaction increased. The evolution of the differential heats with NH_3 uptake shows, indeed, a redistribution of the sites strength in comparison to untreated pristine sample (1.8Al-Sep) with increasing number of medium (160 > Q > 120 kJ/mol) and strong (> 160 kJ/mol) sites. For zeolite materials, post-synthesis treatments—including high-temperature calcination, acid-base leaching (Soh et al., 2017; Chen et al., 2022), and steaming (either in vapor (Corma et al., 2012) or liquid phase (Ravenelle et al., 2010))—are commonly employed to generate more extra-framework and framework-associated aluminum species, such as Al^{3+}, $Al(OH)^{2+}$, $Al(OH)_3$, and Al_2O_3, each exhibiting a different acidity (Batool et al., 2024). Similarly, in sepiolites, the distribution of acid sites (mostly related to the amount and the specific environment of aluminum cations) is modified by acid- or hot water- treatment.

All catalysts showed heterogeneous acidity with a systematic decrease in differential heats with surface coverage (Fig. 6B), indicating the presence of different types of active sites exhibiting various strengths. The site densities in Table S5 are in reasonable agreement with the Al content (1.5, 2.7, and 2.6 Al sites/nm^2 for 0.9Al-Sep, 1.2Al-Sep and Water-1.8Al-Sep, respectively, calculated from chemical analyses in Table 1) except for 1.8Al-Sep (4.4 Al sites/nm^2). Assuming that ammonia adsorbs stoichiometrically on acid sites and that the acid sites in sepiolites pretreated at 400 °C under vacuum (more than two of four coordinated water molecules in a sepiolite unit cell could be removed in this conditions) are generated by Al species, it is likely that not all Al sites in 1.8Al-Sep are accessible for adsorption.

The adsorption of isopropanol (IPA, kinetic diameter 0.47 nm) was first investigated at 75 °C under flow conditions by injecting successive pulses of 1.15 µmol IPA in a continuous He stream over the sample placed in a microcalorimeter. Fig. 7 shows the differential heats of IPA adsorption at 75 °C together with the evolution of IPA uptake as a function of the number of injected pulses.

A continuous decrease in uptake is observed up to the fourth pulse, after which a constant value of 0.11 ± 0.01 µmol/m^2 is reached for all samples (Fig. 7A). The corresponding differential heat profiles follow a similar trend (Fig. 7B). The important change in slope after the fourth pulse may indicate the saturation of the strongest acid sites. The amount of IPA remaining bound to the surface and the corresponding fraction of occupied sites are summarized in Table S6. Assuming that, at low coverage (up to pulse 4), each IPA molecule is strongly anchored at a definite point of the lattice, the surface occupied roughly corresponds to the surface coverage of ammonia adsorbed on acid sites with strengths superior to 80 kJ/mol (Table S5, column 5).

Interestingly, at this coverage, the number of adsorbed IPA molecules corresponds to about half the number of acid sites titrated by NH_3. This indicates either steric limitations of IPA or the involvement of different site configurations for NH_3 and IPA chemisorptions.

The surface chemical interaction is determined by the adsorption temperature and probe strength. In gas phase, NH_3 is a stronger base than isopropanol (ammonia has a proton affinity of about 853.6 kJ/mol versus 793.0 kJ/mol for IPA). On the other hand, the adsorption is favored at lower temperature. Because IPA adsorption is carried out under a continuous He flow, weak acid sites cannot be quantified, in

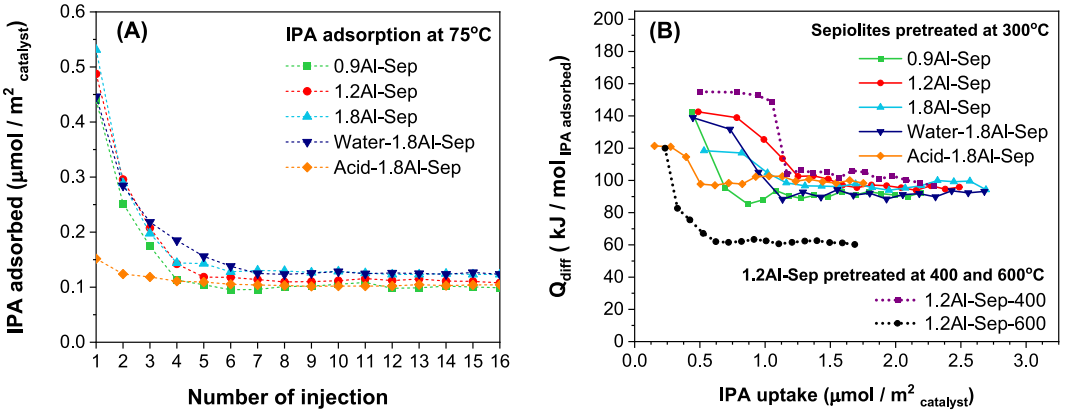

Fig. 7. (A) Pulse-by-pulse evolution of the amount of IPA adsorbed (B) Differential heats of adsorption versus IPA uptake per m^2 of solids. Before adsorption, all samples were pretreated at 300 °C under He flow (30 mL/min). The pulses were introduced at 90 min interval to ensure the equilibrium.

contrast to static NH_3 titration. At low coverage (first four pulses), the decrease in differential heats with increasing IPA uptake reflects surface energetic heterogeneity in pristine and hydrothermally treated samples. All solids were pretreated at 300 °C prior to IPA adsorption and exposed both Brønsted and Lewis acid sites, accounting for acid sites of different strengths. Moderately strong Brønsted acid sites for IPA adsorption (140–110 kJ/mol) may arise from the highly polarized water molecules still bonded to the octahedral Al and the hydroxy-groups generated by heating. The strength of some Brønsted sites could also be affected by the presence nearby of a Lewis acid center contributing to the observed energetic heterogeneity. Lower initial adsorption heats are measured for 1.8Al-Sep in comparison with the other sepiolites, in agreement with NH_3 adsorption microcalorimetry findings. In Acid-1.8Al-Sep, IPA likely interacts preferentially with Brønsted Si–O(H)–Al groups in the amorphous silica framework, giving adsorption heats of ~120 kJ/mol.

The distribution of surface sites is strongly affected by the pretreatment temperature. For clarity, Fig. 7B shows results for only 1.2Al-Sep pretreated at 400 and 600 °C. After pretreatment at 400 °C, sepiolites exhibit a plateau around 150 kJ/mol, characteristic of a homogeneous population of strong sites. In contrast, pretreatment at 600 °C leads to a marked decrease in IPA uptake and a rapid drop in initial adsorption heat from ~120 to ~80 kJ/mol, followed by a gradual decrease to ~60 kJ/mol, indicating significant changes in acid-sites nature and strength.

From the 5th pulse onwards, all IPA adsorption was essentially reversible and independent of coverage. This reversible uptake is attributed to terminal silanol groups and exposed unsaturated cations, as similar values are obtained for Acid-1.8Al-Sep and untreated pristine sepiolites. The average value of 96 ± 4 kJ/mol found for the differential heats at the reversible equilibrium plateau relates to medium strength sites. This value remains nearly the same for the samples pretreated at 300 or 400 °C while a pretreatment at 600 °C shows a huge decrease of the value of this plateau to about 60 kJ/mol. This behavior relates to the complete loss of the coordination water molecules and the collapse of the sepiolite structure at 600 °C. The residual silanol groups may act as active sites for the isopropanol adsorption (the adsorption of water on silanol groups of silica gives rise to adsorption heats of about 50 kJ/mol (Busca, 2019)).

3.4. IPA dehydration reaction and the correlation to catalysts properties

After IPA saturation at 75 °C, the microreactor temperature was increased over the range of 100 to 300 °C. Catalysts were contacted, at each selected temperature, with 6 successive pulses of IPA (1.15 μmol) under continuous He flow. IPA conversion and products distribution, calculated from the 6th pulse at each temperature, provide insight into the catalytic activity of the sepiolites (Table S7 and Fig. 8). The isopropanol dehydration leads to (i) propylene (PEN) which formation is expected to increase with acidic character of the catalyst and (ii) diisopropyl ether (DIPE) produced on weak acid sites, thermodynamically favored at low temperatures. The IPA dehydrogenation to acetone relates to the synergetic effect of acidic and basic sites on a surface. Regarding the predominant acid properties of sepiolites, the dehydrogenation reaction is not expected at low temperatures.

Below 200 °C, dehydration was the only reaction observed, with conversion increasing with temperature, consistent with the endothermic nature of the process. At these low reaction temperatures, not all adsorbed IPA is neither activated for catalytic conversion or desorbed, probably due to a strong chemisorption of IPA (Q > 140 kJ/mol, Fig. 7B). Inactivated IPA in Fig. 8 includes the remaining adsorbed species on the catalyst in one form or another, mostly present at low reaction temperature. This generates a pool of reagent adsorbed on the surface and available for the reaction.

The less active 0.9Al-Sep (reference, less acidic sepiolite) showed <4% conversion at 125 °C and ~ 60% at 200 °C, whereas 1.2Al- and 1.8Al-Sep were active from 100 °C. Propylene (PEN) was the main product with selectivity above 90% at all temperatures, while DIPE was a minor product whose selectivity decreased with temperature. Acid-1.8Al-Sep exhibits the lowest and nearly linear increase in IPA conversion with temperature, consistent with its very low density of active acid sites after amorphization. Water-1.8Al-Sep, despite a loss of Al after water-leaching, shows a catalytic activity comparable to the untreated parent sepiolite. During the reaction, generated water may induce local hydration–dehydration processes, making also this hydrothermal treatment relevant for simulating catalyst aging. The results indicate that produced water by the reaction has little impact on catalytic performances of sepiolites. In the absence of Al leaching, water mainly reduces Lewis acidity without significantly affecting Brønsted sites (Postole et al., 2025). Notably, at similar IPA conversions (52–56% at 125 °C), DIPE formation is negligible over Water-1.8Al-Sep, unlike untreated pristine samples, indicating changes in acid-site distribution induced by hydrothermal treatment, in agreement with NH_3 adsorption microcalorimetry (Fig. 6).

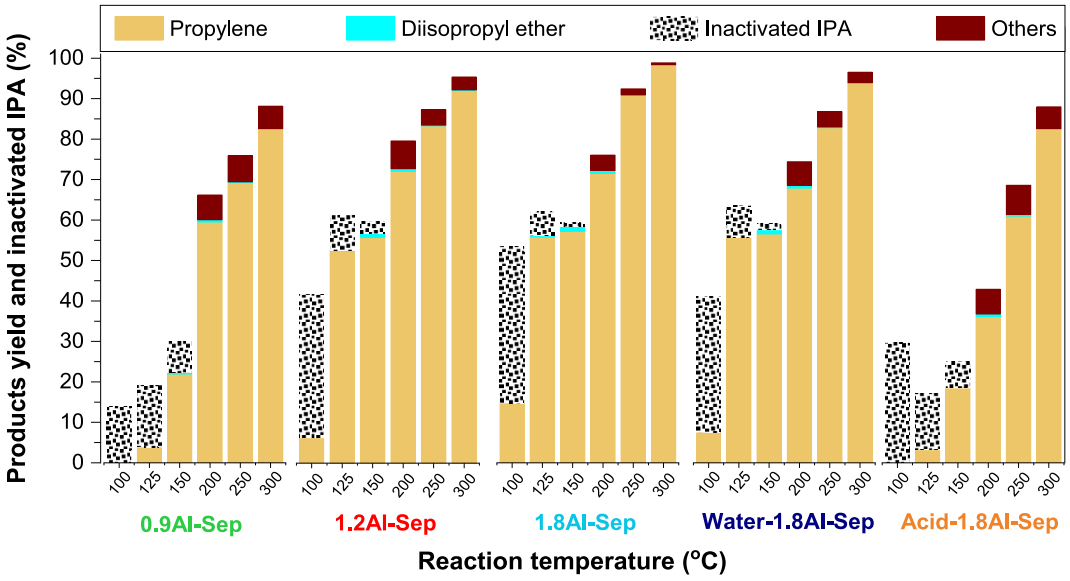

Fig. 8. Yields of products and inactivated IPA over sepiolite catalysts versus reaction temperature. The *inactive IPA* was calculated as ($n_{IPA,in} - n_{IPA,out} - n_{PEN} - 2xn_{DIPE}$) up to 150 °C. Between 200 and 300 °C *Others* contain the side-reactions products and the inactivated IPA.

Fig. 9A shows direct correlation between Al content and the number of acid sites determined by NH_3 adsorption microcalorimetry (Fig. 6A, Table S5), excluding Acid-1.8Al-Sep due to amorphization. The correlation shows the important contribution of Al to catalytically relevant acidity.

Water treatment reduces the Al content of 1.8Al-Sep to a level close to that of 1.2Al-Sep, explaining their similar catalytic performances and supporting the correlation. Moreover, catalytic activity at 125 and 150 °C was found to correlate with the number of medium–strong acid sites ($Q_{diff\ NH3} > 80$ kJ/mol) (Fig. 9B), highlighting the importance of acid strength in addition to site density for IPA dehydration. This suggests that acid sites with strength >80 kJ/mol are most catalytically relevant to the performance of sepiolite at low temperatures.

IPA conversion continues to increase at higher temperatures, while PEN selectivity decreases due to by-products formation (≥200 °C for 1.2Al-, 1.8Al- and Water-1.8Al-Sep; ≥250 °C for 0.9Al- and Acid-1.8Al-Sep). Trace acetone is detected between 200 and 300 °C, consistent with residual basicity, with the 0.9Al-Sep sample producing the highest amount (Fig. S11). Other hydrocarbon by-products (propane, higher oligomers arising from PEN olygomerization) formed at intermediate temperatures lead to some coke deposition and reduced PEN selectivity (Fig. S12), but become low at 300 °C, where 1.8Al-Sep reaches 99% conversion and PEN selectivity. However, operating at lower temperatures (e.g., 150 °C) is more advantageous, as it requires lower energy cost while providing high propylene selectivity without no structural degradation of sepiolote. High selectivity at low temperature may be attributed to site isolation by strongly adsorbed IPA which can limit possible oligomerization.

Catalytic activity also strongly depends on thermal activation temperature, as seen in Fig. 10 for 1.2Al-Sep as an example. Activation at 200 °C leads to the highest activity, as the removal of physisorbed water enhances the accessibility of active sites. Further activation between 250 and 400 °C leads to progressive activity loss due to the diminution of Al-coordinated water sites, while pretreatment at 600 °C provokes a structural collapse and a huge loss of activity, thus highlighting the critical role of activation temperature in controlling acidity and structure. These results are strongly consistent with the NH_3-FTIR conclusions previously discussed.

In summary, 1.2Al-Sep and 1.8Al-Sep combine Brønsted and Lewis acidities with good thermal stability and textural properties, resulting in high conversion and selectivity. Water-1.8Al-Sep exhibits comparable activity due to a similar Al environment, whereas the 0.9Al-Sep samples, with lower Al content and weaker Brønsted acidity, shows inferior performance. Acid treatment of 1.8Al-Sep leads to amorphization, loss of Brønsted acidity and reduced activity at low temperature. Besides reaction-generated water may dynamically improve acidity and activity at higher temperatures.

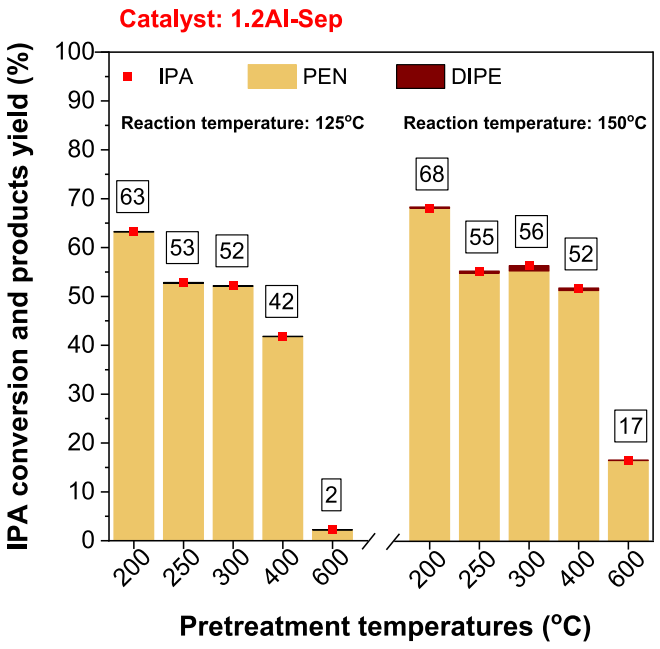

Fig. 10. IPA conversion of 1.2Al-Sep pretreated at 200, 250, 300, 400 and 600 °C. At 600 °C, based on TGA and NMR data, the desorption of all coordinated-water molecules is expected to occur and bridging silanol proton remained intact.

This study demonstrates the relevance of using natural sepiolites as catalysts for isopropanol to propylene reaction. Investigated sepiolites exhibit better performances at lower temperatures when comparing with clays reported in literature, although a rigorous comparison of the data is difficult due to the variety of experimental conditions (temperature, pressure, reactant gas composition) and clays characteristics (exposed sites, nature of alkali metal cations). Synthesized saponites in (Sychev and Prihod'ko, 1998) showed only moderate IPA conversion (~30–40% at 200 °C) with limited propylene selectivity. The saponites studied in (Kawi and Yao, 1999) were largely inactive for IPA dehydration unless fully substituted with Ni. Hectorite and hectorite-like minerals prepared by (Suzuki et al., 1988), in which the Na cations were replaced by other alkali metal cations, exhibited maximum 20% isopropanol conversion and 16% yield of PEN at 250 °C.

These results indicate that the fibrous sepiolite structure provides an efficient acidic environment for IPA dehydration.

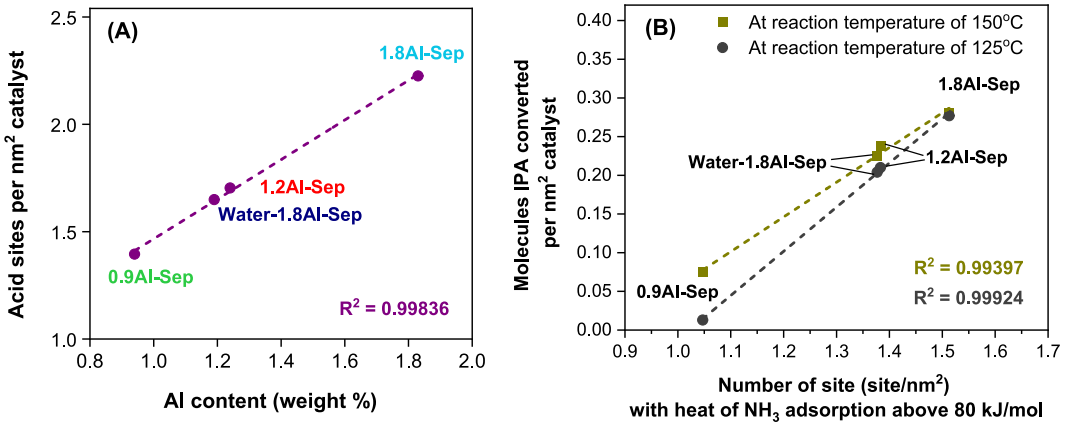

Fig. 9. (A) Correlation between Al content in the catalysts and the number of acid sites determined by adsorption microcalorimetry at total NH_3 uptake at 27 Pa. (B) Correlation between the number of medium-strong acid sites present in the catalysts and their IPA conversion at low reaction temperature (125 and 150 °C).

4. Conclusion

The acidity of sepiolite catalysts containing low amounts of Al was thoroughly characterized by combining NH_3 adsorption microcalorimetry, NH_3-FTIR, and solid-state NMR. The presence of Al was shown to generate both bridging silanols and Al-coordinated water sites, beneficial to isopropanol dehydration, while thermal treatment produced coordinatively unsaturated Al species that act as Lewis acid sites. The relationship between Al content, acidity, and catalytic performance has been clearly established. The water or acid modified 1.8Al-Sep samples showed that the sepiolite activity was significantly impacted by small variations in Al content and coordination environment. In clays, residual basicity was found to promote acetone formation, emphasizing that suitable acidity combined with low basicity is essential for high propylene selectivity. Porosity and structural stability must be also considered for tunning the fibrous sepiolite properties for application in catalysis. Sepiolite can be considered as a promising, natural low-cost catalyst for acid-catalyzed isopropanol dehydration at low temperatures, offering an alternative route to propylene production that complements conventional petrochemical pathways.

Authors contribution

The manuscript was written through contributions of all authors. All authors have given approval to the final version of the manuscript.

CRediT authorship contribution statement

Tien Hoang Nguyen: Writing – original draft, Methodology, Investigation, Formal analysis, Conceptualization. **Jean-Luc Dubois:** Writing – review & editing, Validation. **Aline Auroux:** Writing – review & editing, Validation. **Georgeta Postole:** Writing – review & editing, Validation, Supervision, Project administration, Methodology, Conceptualization.

Declaration of competing interest

The authors declare that they have no known competing financial interests or personal relationships that could have appeared to influence the work reported in this paper.

Acknowledgment

This work is part of PYROCO2 project that has received funding from the European Union's Horizon 2020 Research and Innovation Program under grant agreement No. 101037009.

Special thanks are addressed to the technical services of IRCELYON (Institut de Recherches sur la Catalyse et l'Environnement de Lyon): Chantal Lorentz, Nicolas Bonnet, Pascal Mascunan, Yoann Aizac, Pierre Martinez-Ginouvès and Laurence Burrel for valuable technical contributions in XRD, NMR, SEM, TEM and chemical analysis.

Appendix A. Supplementary data

Electron microscopy images; pore size distributions; supplementary solid NMR data; FTIR spectra; evolution of BET surface area with temperature; TGA-FTIR data; supplementary calorimetric data (NH_3/IPA); IPA conversion values; GC signals of outlet gaseous mixture at different temperatures. Supplementary data to this article can be found online at [https://doi.org/10.1016/j.clay.2026.108232].

Data availability

Data will be made available on request.

References

Abeyta, K.P., Silva, M.L.A.D., Silva, C.L.S., Pontes, L.A.M., Teixeira, L.S.G., 2024. Clay-based catalysts applied to glycerol valorization: a review. Sustain. Chem. Pharm. 40, 101641. https://doi.org/10.1016/j.scp.2024.101641.

Al-Ani, A., Gertisser, R., Zholobenko, V., 2018. Structural features and stability of Spanish sepiolite as a potential catalyst. Appl. Clay Sci. 162, 297–304. https://doi.org/10.1016/j.clay.2018.06.021.

Aramendía, M.A., Borau, V., Jiménez, C., Marinas, J.M., Ruiz, J.R., 1997. Characterization of Spanish sepiolites by high-resolution solid-state NMR. Solid State Nucl. Magn. Reson. 8, 251–256. https://doi.org/10.1016/S0926-2040(97)00009-X.

Aribert, N., Brandhorst, L., Coupard, V., Maury, S., Vivien, T., 2014. Method for dehydrating a mixture containing ethanol and isopropanol. In: European Patent EP3074369. Assigned to IFP Energies Nouvelles. https://worldwide.espacenet.com/patent/search/family/049998514/publication/EP3074369A1?q=EP3074369.

Auroux, A., 1994. In: Imelik, B., Védrine, J.C. (Eds.), Catalysts Characterization: Physical Techniques for Solid Materials. Plenum Press, New York, p. 611.

Balestra, G., De Maron, J., Tabanelli, T., Cavani, F., Nieto, J.M.L., 2023. The selective ethanol Guerbet condensation over alkali metal-doped sepiolite. Catal. Today 423, 114013. https://doi.org/10.1016/j.cattod.2023.01.020.

Barrett, E.P., Joyner, L.G., Halenda, P.P., 1951. The determination of pore volume and area distributions in porous substances. I. Computations from nitrogen isotherms. J. Am. Chem. Soc. 73 (1), 373–380. https://doi.org/10.1021/ja01145a126.

Batool, S.R., Sushkevich, V.L., Van Bokhoven, J.A., 2024. Factors affecting the generation and catalytic activity of extra-framework aluminum Lewis acid sites in Aluminum-Exchanged zeolites. ACS Catal. 14, 678–690. https://doi.org/10.1021/acscatal.3c04195.

Belaroui, L.S., Bengueddach, A., 2012. Study of the catalytic activity of Al-Fe pillared clays in the Baeyer–Villiger oxidation. Clay Miner. 47, 275–284. https://doi.org/10.1180/claymin.2012.047.2.10.

Belver, C., Aranda, P., Ruiz-Hitzky, E., 2013. Silica–alumina/sepiolite nanoarchitectures. J. Mater. Chem. A 1, 7477. https://doi.org/10.1039/c3ta01686b.

Bergaya, F., Lagaly, G., 2013. Handbook of Clay Science, Second edition. Developments in Clay Science. Elsevier, Amsterdam.

Bisio, C., Gatti, G., Boccaleri, E., Marchese, L., Superti, G.B., Pastore, H.O., Thommes, M., 2008. Understanding physico–chemical properties of saponite synthetic clays. Microporous Mesoporous Mater. 107, 90–101. https://doi.org/10.1016/j.micromeso.2007.05.038.

Brunauer, S., Emmett, P.H., Teller, E., 1938. Adsorption of gases in multimolecular layers. J. Am. Chem. Soc. 60 (2), 309–319. https://doi.org/10.1021/ja01269a023.

Busca, G., 2019. Catalytic materials based on silica and alumina: Structural features and generation of surface acidity. Prog. Mater. Sci. 104, 215–249. https://doi.org/10.1016/j.pmatsci.2019.04.003.

Cabanis, T., Auroux, A., Dubois, J.-L., Sbirrazzuoli, N., Postole, G., 2025. An innovative approach to evidence pathways in a reactional mechanism of heterogenous catalysis. Appl. Catal. O Open 208, 207073. https://doi.org/10.1016/j.apcato.2025.207073.

Casal, B., Merino, J., Ruiz-Hitzky, E., Alvarez, A., Gutierrez, E., 1996. Characterization, pillaring and catalytic properties of a saponite from Vicalvaro, Madrid, Spain. Clay Miner. 32, 41–54. https://doi.org/10.1180/claymin.1997.032.1.06.

Chen, Q., Zhu, R., Liu, S., Wu, D., Fu, H., Zhu, J., He, H., 2018. Self-templating synthesis of silicon nanorods from natural sepiolite for high-performance lithium-ion battery anodes. J. Mater. Chem. A 6, 6356–6362. https://doi.org/10.1039/C8TA00587G.

Chen, H., Geng, J., Zhang, Z., Jiang, R., Zhai, J., Zhang, J., 2021. The structure and properties of Sepiolite with partial lattice ions substituted by aluminum ions. Front. Chem. 9, 721225. https://doi.org/10.3389/fchem.2021.721225.

Chen, K., Zornes, A., Bababrik, R., Crouch, J., Alvarez, W., Wulfers, M., Resasco, D., Wang, B., Crossley, S., White, J.L., 2022. First-formed framework species and phosphate structure distributions in Phosphorus-Modified MFI zeolites. J. Phys. Chem. C 126, 227–238. https://doi.org/10.1021/acs.jpcc.1c08448.

Chevalier, S., Franck, R., Suquet, H., Lambert, J.-F., Barthomeuf, D., 1994. Al-Pillared saponites. Part 1.—IR studies. J. Chem. Soc. Faraday Trans. 90, 667–674. https://doi.org/10.1039/FT9949000667.

Chizallet, C., Raybaud, P., 2009. Pseudo-Bridging silanols as versatile brønsted acid sites of amorphous aluminosilicate surfaces. Angew. Chem. 121, 2935–2937. https://doi.org/10.1002/ange.200804580.

Chizallet, C., Raybaud, P., 2010. Acidity of amorphous Silica–Alumina: from coordination promotion of Lewis sites to proton transfer. ChemPhysChem 11, 105–108. https://doi.org/10.1002/cphc.200900797.

Corma, A., Pérez-Pariente, J., 1987. Catalytic activity of modified silicates: I. Dehydration of ethanol catalysed by acidic sepiolites. Clay Miner. 22, 423–433. https://doi.org/10.1180/claymin.1987.022.4.06.

Corma, A., Perez-Pariente, J., Fornes, V., Mifsud, A., 1984. Surface acidity and catalytic activity of a modified sepiolite. Clay Miner. 19, 673–676. https://doi.org/10.1180/claymin.1984.019.4.14.

Corma, A., Pérez-Pariente, J., Soria, J., 1985. Physico-chemical characterization of Cu 2 + −exchanged sepiolite. Clay Miner. 20, 467–475. https://doi.org/10.1180/claymin.1985.020.4.03.

Corma, A., Mengual, J., Miguel, P.J., 2012. Steam catalytic cracking of naphtha over ZSM-5 zeolite for production of propene and ethene: micro and macroscopic implications of the presence of steam. Appl. Catal. A Gen. 417–418, 220–235. https://doi.org/10.1016/j.apcata.2011.12.044.

Del Rio, M.S., Garcia-Romero, E., Suarez, M., Da Silva, I., Fuentes-Montero, L., Martinez-Criado, G., 2011. Variability in sepiolite: diffraction studies. Am. Mineral. 96, 1443–1454. https://doi.org/10.2138/am.2011.3761.

D'Espinose De La Caillerie, J.-B., Fripiat, J.J., 1992. AL modified Sepiolite as catalyst or catalyst support. Catal. Today 14, 125–140. https://doi.org/10.1016/0920-5861(92)80017-H.

D'Espinose De La Caillerie, J.B., Gruver, V., Fripiat, J.J., 1995. Modification of the surface properties of natural phyllosilicate Sepiolite by secondary isomorphic substitution. J. Catal. 151, 420–430. https://doi.org/10.1006/jcat.1995.1044.

Dontsova, K.M., Norton, L.D., Johnston, C.T., 2005. Calcium and magnesium effects on ammonia adsorption by soil clays. Soil Sci. Soc. Am. J. 69, 1225–1232. https://doi.org/10.2136/sssaj2004.0335.

Dubois, J.-L., Postole, G., Silvester, L., Auroux, A., 2022. Catalytic dehydration of isopropanol to propylene. Catalysts 12, 1097. https://doi.org/10.3390/catal12101097.

Figueras, F., 1988. Pillared clays as catalysts. Catal. Rev. 30, 457–499. https://doi.org/10.1080/01614948808080811.

Fois, G.A., Buzzoni, R., 2018. Process for Producing Olefins from Alcohols. PCT Patent Application WO 2019/008499.2 Assigned to VERSALIS S.P.A. https://worldwide.espacenet.com/patent/search/family/060202348/publication/WO2019008499A1?q=WO%202019%2F008499.

Fukuhara, H., Matsunaga, F., Yasuhara, M., Araki, S., Isaka, T.I., 1989. Preparation of propylene. In: Assigned to MITSUI Petrochemical Industries Ltd (Ed.), European Patent EP0379803. https://worldwide.espacenet.com/patent/search/family/026547935/publication/EP0379803A1?q=EP0379803.

Gervasini, A., Fenyvesi, J., Auroux, A., 1997. Study of the acidic character of modified metal oxide surfaces using the test of isopropanol decomposition. Catal. Lett. 43, 219–228. https://doi.org/10.1023/A:1018979731407.

Jiang, Y., Huang, J., Dai, W., Hunger, M., 2011. Solid-state nuclear magnetic resonance investigations of the nature, property, and activity of acid sites on solid catalysts. Solid State Nucl. Magn. Reson. 39, 116–141. https://doi.org/10.1016/j.ssnmr.2011.03.007.

Kawi, S., Yao, Y.Z., 1999. Saponite catalysts with systematically varied Mg/Ni ratio: synthesis, characterization, and catalysis. Microporous Mesoporous Mater. 33, 49–59. https://doi.org/10.1016/S1387-1811(99)00122-5.

Larmier, K., Chizallet, C., Maury, S., Cadran, N., Abboud, J., Lamic-Humblot, A., Marceau, E., Lauron-Pernot, H., 2017. Isopropanol dehydration on amorphous Silica–Alumina: synergy of Brønsted and Lewis acidities at Pseudo-Bridging Silanols. Angew. Chem. Int. Ed. 56, 230–234. https://doi.org/10.1002/anie.201609494.

Marosz, M., Kowalczyk, A., Gil, B., Chmielarz, L., 2020. Acid-treated clay minerals as catalysts for dehydration of methanol and ethanol. Clay Clay Miner. 68, 23–37. https://doi.org/10.1007/s42860-019-00051-y.

Ouali, A., Belaroui, L.S., Bengueddach, A., Galindo, A.L., Peña, A., 2015. Fe2O3–palygorskite nanoparticles, efficient adsorbates for pesticide removal. Appl. Clay Sci. 115, 67–75. https://doi.org/10.1016/j.clay.2015.07.026.

Pérez Pariente, J., Fornés, V., Corma, A., Mifsud, A., 1988. The surface acidity and hydrothermal stability of Sepiolite derivatives. Appl. Clay Sci. 3, 299–306. https://doi.org/10.1016/0169-1317(88)90021-X.

Phung, T.K., Busca, G., 2015. On the Lewis acidity of protonic zeolites. Appl. Catal. A Gen. 504, 151–157. https://doi.org/10.1016/j.apcata.2014.11.031.

Plee, D., Fripiat, J.J., Schutz, A., Poncelet, G., 1985. Acid properties of a Bidimensional Zeolite. In: Studies in Surface Science and Catalysis. Elsevier, pp. 343–350. https://doi.org/10.1016/S0167-2991(09)60184-1.

Plee, D., Gatineau, L., Fripiat, J.J., 1987. Pillaring processes of smectites with and without tetrahedral substitution. Clay Clay Miner. 35, 81–88. https://doi.org/10.1346/CCMN.1987.0350201.

Portela, R., Rubio-Marcos, F., Leret, P., Fernández, J.F., Bañares, M.A., Ávila, P., 2015. Nanostructured ZnO/Sepiolite monolithic sorbents for h2s removal. J. Mater. Chem. A 3, 1306–1316. https://doi.org/10.1039/C4TA04440A.

Postole, G., Segondy, S., Cabanis, T., Nguyen, T.-H., Auroux, A., Dubois, J.-L., 2025. Relationship between number and strength of acid–base catalytic sites and their performances in isopropanol dehydration reaction. Catalysts 15, 768. https://doi.org/10.3390/catal15080768.

Ravenelle, R.M., Schüβler, F., D'Amico, A., Danilina, N., Van Bokhoven, J.A., Lercher, J. A., Jones, C.W., Sievers, C., 2010. Stability of zeolites in hot liquid water. J. Phys. Chem. C 114, 19582–19595. https://doi.org/10.1021/jp104639e.

Ruiz, A.I., Ruiz-García, C., Ruiz-Hitzky, E., 2023. From old to new inorganic materials for advanced applications: the paradigmatic example of the Sepiolite clay mineral. Appl. Clay Sci. 235, 106874. https://doi.org/10.1016/j.clay.2023.106874.

Soh, J.C., Chong, S.L., Hossain, S.S., Cheng, C.K., 2017. Catalytic ethylene production from ethanol dehydration over non-modified and phosphoric acid modified zeolite H-Y (80) catalysts. Fuel Process. Technol. 158, 85–95. https://doi.org/10.1016/j.fuproc.2016.12.012.

Sun, A., d'Espinose De La Caillerie, J.-B., Fripiat, J.J., 1995. A new microporous material: aluminated Sepiolite. Microporous Mater. 5, 135–142. https://doi.org/10.1016/0927-6513(95)00049-F.

Suzuki, E., Idemura, S., Ono, Y., 1988. Catalytic conversion of 2-propanol and ethanol over synthetic hectorite and its analogues. Appl. Clay Sci. 3, 123–134. https://doi.org/10.1016/0169-1317(88)90012-9.

Sychev, M., Prihod'ko, R., 1998. Characterization and catalytic activity of non-hydrothermally synthesized saponite-like materials. In: Studies in Surface Science and Catalysis. Elsevier, pp. 967–974. https://doi.org/10.1016/S0167-2991(98)80265-6.

Wang, Z., Jiang, Y., Lafon, O., Trébosc, J., Duk Kim, K., Stampfl, C., Baiker, A., Amoureux, J.-P., Huang, J., 2016. Brønsted acid sites based on penta-coordinated aluminum species. Nat. Commun. 7, 13820. https://doi.org/10.1038/ncomms13820.

Zhou, C.H., Li, G.L., Zhuang, X.Y., Wang, P.P., Tong, D.S., Yang, H.M., Lin, C.X., Li, L., Zhang, H., Ji, S.F., Yu, W.H., 2017. Roles of texture and acidity of acid-activated sepiolite catalysts in gas-phase catalytic dehydration of glycerol to acrolein. Mol. Catal. 434, 219–231. https://doi.org/10.1016/j.mcat.2016.12.022.